Carbohydrate Polymers 90 (2012) 887–893

Contents lists available at SciVerse ScienceDirect

Carbohydrate Polymers

journal homepage: www.elsevier.com/locate/carbpol

Efficient removal of both cationic and anionic dyes from aqueous solutions using a novel amphoteric straw-based adsorbent

Wenxuan Zhang[a], Hu Yang[a,*], Lei Dong[a], Han Yan[a], Haijiang Li[a], Ziwen Jiang[a], Xiaowei Kan[a], Aimin Li[a], Rongshi Cheng[a,b]

[a] State Key Laboratory of Pollution Control and Resource Reuse, School of the Environment, School of Chemistry & Chemical Engineering, Nanjing University, Nanjing 210093, PR China
[b] Polymer Institute, College of Material Science and Engineering, South China University of Technology, Guangzhou 510640, PR China

ARTICLE INFO

Article history:
Received 24 February 2012
Received in revised form 17 May 2012
Accepted 10 June 2012
Available online 17 June 2012

Keywords:
Amphoteric straw-based adsorbent
Adsorption of both cationic and anionic dyes
Adsorption mechanism
Wastewater treatment

ABSTRACT

In the current paper, a novel amphoteric straw-based adsorbent was prepared and applied to adsorb various dyes from aqueous solutions. The amphoteric adsorbent was proven effective in eliminating both cationic and anionic dyes (methylene blue and acid green 25), especially at corresponding favored pH conditions. The fundamental adsorption behavior of the adsorbent on removing various dyes was also investigated at different temperatures. The adsorption isotherms were all best-fitted by the Langmuir equation, whereas the adsorption kinetics was well-described by both the pseudo-second order model and the Elovich model. The experimental result revealed that the adsorption mechanism followed the monolayer chemical adsorption with an ion-exchange process.

1. Introduction

To date, water pollution is attracting increasing concerns due to the rapid industrial development in China. Dyes, as main pollutants in industrial sewage, are not only unpleasant to the eyes, but also harmful for the living organisms in the biosphere. Colored dye effluents may interfere with light penetration in the receiving water bodies, thereby disturbing the biological processes (Tsai et al., 2007). In addition, some dyes degrade into toxic, mutagenic, or carcinogenic compounds that have harmful influences on ecosystem (O'Neill et al., 1999).

Various techniques, including adsorption (Ngah, Teong, & Hanafiah, 2011), flocculation (Zahrim, Tizaoui, & Hilal, 2011), oxidation (Serpone, Horikoshi, & Emeline, 2010), and electrolysis (Vandevivere, Bianchi, & Verstraete, 1998), have been employed to eliminate dyes from wastewaters. Among these methods, adsorption is the most commonly applied because it is more efficient and economical than the others. Recently, many biological materials, especially agricultural residues, including peanut hull (Tanyildizi, 2011), sugarcane bagasse (Yu, Chi, He, & Qi, 2011), coir pith (Khan, Ray, & Guha, 2011), and maize cob (Sonawane & Shrivastava, 2009), have been applied as adsorbents for dyestuff removal.

However, more than 300 million tons of straw are incinerated or deserted in China annually. The heat of burning straw kills microorganisms and brings damage to the ecological equilibrium in the soil. Even worse, emissions from straw burning, which comprise various contaminants, are transported and mixed with other urban pollutants, resulting in haze events (Li et al., 2007; Wang et al., 2009; Zhang, Tao, Cao, & Coveney, 2007). People have recently begun to realize the harmful effects of burning straw and thus began considering many ways to use this bioresource. Straw is rich in various natural polymer materials, such as cellulose and lignin, which have been applied to produce various products, namely, particleboards (Binod et al., 2010), paper (Rafatullah, Sulaiman, Hashim, & Ahmad, 2010), fuel (Kuang, Kuang, Zheng, & Wang, 2010), adsorbents (Hou et al., 2011), and so on.

Among these applications, using straw as adsorbent is a promising alternative for the removal of dyes in wastewater treatment due to its very low cost. However, raw straw is deficient in functional groups which are capable of adsorbing ionic dyes through electrostatic interaction. Accordingly, the removal efficiency of raw straw is unsatisfactory (Abdel-Aal, Gad, & Dessouki, 2006). Therefore, ionic groups are introduced into the straw through chemical modification to improve its adsorption capacity. Anionic straw has been prepared and proven effective in eliminating cationic dyes (Gong, Jin, Chen, Chen, & Liu, 2006; Gong, Zhong, Hu, Chen, & Zhu, 2008; Zhang et al., 2011). On the other hand, cationic straw is advantageous for the removal of anionic dyes (Ibrahim, Fatimah,

* Corresponding author. Tel.: +86 25 83686350; fax: +86 25 83686350.
E-mail address: yanghu@nju.edu.cn (H. Yang).

0144-8617/$ – see front matter © 2012 Elsevier Ltd. All rights reserved.
http://dx.doi.org/10.1016/j.carbpol.2012.06.015

Ang, & Wang, 2010; Ibrahim, Shuy, Ang, & Wang, 2010; Oei, Ibrahim, Wang, & Ang, 2009; Xu, Gao, Yue, & Zhong, 2010). However, the content of industrial sewage is normally complicated, and adsorption using only one type of ionic group is usually incapable of eliminating various ionic dyes. One sort of adsorbent with both cationic and anionic groups is required to realize the adsorption of both anionic and cationic dyes. However, to date, very little work has been focused on amphoteric adsorbents.

In the current research, quaternary ammonium and carboxymethyl groups are successively introduced to wheat straw, from which a novel amphoteric adsorbent is prepared. The adsorbent is then used for the removal of methylene blue, a kind of cationic dye, and acid green 25, a kind of anionic dye, from aqueous solutions. The fundamental adsorption behavior of the adsorbent, including the effects of pH, adsorption equilibrium, and kinetics, are investigated. The new adsorbent is proven effective in eliminating both cationic and anionic dyes, especially at corresponding favored pH conditions. The adsorption mechanisms of the adsorbent are also discussed in detail.

2. Materials and methods

2.1. Materials

The wheat straw used in the present study was obtained from a farm in Changzhou, Jiangsu Province, China. Methylene blue (MB), acid green 25 (AG25), chloroactic acid, 3-chloro-2-hydroxypropyl trimethylammonium chloride (CTA), hydrochloric acid (HCl), sodium hydrate (NaOH), ethanol, isopropanol, and other reagents used in the current work were all A.R.-grade reagents. Distilled water was used in all experiments.

2.2. Preparation of the biosorbent

The synthesis of amphoteric wheat straw is summarized in Scheme 1. The straw materials were ground and screened through a set of sieves to obtain geometrical sizes of around 60–150 μm. The sieved straw was then washed with ethanol and distilled water. The washed materials were dried in an oven at 353 K for 24 h. The straw material used in the current study was named WS.

The desired amount of WS was dispersed in isopropanol and NaOH blending aqueous solution to swell and alkalize. CTA was then added dropwise into the mixture and left under agitation at 318 K for 3 h. A cationic straw-based material resulted. Subsequently, the CTA-grafted straw was transferred into a NaOH alcohol–water solution in which chloroactic acid was added dropwise. The reaction was kept under agitation for 1.5 h at 353 K. Afterward, the modified straw was filtered, washed, and dried. The final product was amphoteric wheat straw (AWS).

In addition, an anionic straw-based material was prepared via carboxymethylation according to our previous work (Zhang et al., 2011) for further comparison.

2.3. Characterization of the biosorbent

The Fourier transform infrared (FTIR) spectra of the various straw-based adsorbents were obtained using a Bruker IFS 66/S IR Spectrophotometer. All samples were prepared as potassium bromide tablets, and the scanning range was 650–4000 cm^{-1}.

The ζ potential data was acquired from a Malvern Nano-Z ζ potential recorder. The range of initial pH was 2.0–10.0.

The amounts of quaternary ammonium and carboxymethyl groups that have been impregnated onto the straw surface were both determined by colloidal titration. Polyvinyl sulfuric acid potassium salt (PVSK) standard solution was applied as volumetric solution and toluidine blue (TB) was used as an indicator. The amount of quaternary ammonium groups could be directly determined by titrating using PVSK solution at pH 2.0, while the amount of carboxymethyl groups could be determined by adding superfluous poly dimethyl diallyl ammonium chloride (PDADMAC) beforehand, and then back-titrating using PVSK standard solution at pH 9.0.

2.4. Adsorption studies

2.4.1. pH variation

The influences of different initial pH to the adsorption of MB and AG25 by WS and AWS were investigated using the batch method. The range of initial pH values was between 2.0 and 10.0. The solution pH was adjusted by 0.1 mol L^{-1} HCl or NaOH aqueous solutions. Approximately 0.03 g adsorbent was immersed into 30 mL dye solution for 48 h at 298 K. The initial concentrations of the MB and AG25 solutions were both approximately 500 mg g^{-1} for each experiment. After reaching the adsorption equilibrium, the dyes and adsorbents aqueous mixtures were settled until the adsorbents were full precipitated. Then the supernatant solution was taken out, and the final concentrations of the MB and AG25 solutions were determined using Vis spectrophotometer (Type 7200; Unico Corp.; China), which were detected at wavelengths of 662 and 642 nm, respectively. Subsequently, the dye uptake q (mg g^{-1}) was calculated using the following equation:

$$q = \frac{(C_0 - C_e)V}{m} \quad (1)$$

where C_0 and C_e (mg L^{-1}) are the initial and equilibrium dye concentrations of the solutions, V (L) is the volume of the solution, and m (g) is the dried weight of the adsorbent.

2.4.2. Adsorption equilibrium study

The adsorption equilibrium studies of AWS for MB and AG25 were both conducted at different dye solution temperatures: 283, 293, 303, and 313 K controlled by a circulating water bath. The concentration of MB aqueous solutions ranged from 25 mg L^{-1} to 500 mg L^{-1}, whereas the concentration of AG25 aqueous solutions ranged from 50 mg L^{-1} to 1000 mg L^{-1}. The initial solution pH of MB and AG25 were adjusted to 10.0 and 3.0, respectively. A desired amount of AWS was weighed and dosed in each dye solution for 48 h. A similar analysis method using the Vis spectrophotometer as mentioned above was employed to detect the initial and final dye concentrations. The dye uptake was calculated based on Eq. (1).

2.4.3. Adsorption kinetics

Adsorption kinetics study was also conducted at different dye solution temperatures: 283, 293, 303, and 313 K controlled by a circulating water bath. The initial concentrations of MB and AG25 solutions were fixed at approximately 500 mg L^{-1} and 600 mg L^{-1}, respectively. The solution pH was adjusted to 10.0 for MB and 3.0 for AG25. About 0.5 g AWS was immersed into a 500 mL dye solution under continuous stirring. About 1 mL of the sample solution was then taken out at desired time intervals to analyze the current dye concentration. Meanwhile, the same volume of water was added into the bulk solution to keep the volume constant. The dye uptake at time t_i, $q(t_i)$ (mg g^{-1}) was calculated using the following equation:

$$q(t_i) = \frac{(C_0 - C_{t_i})V_o - \sum_2^{i-1} C_{t_{i-1}} V_s}{m} \quad (2)$$

where C_0 and C_{t_i} (mg L^{-1}) are the initial dye concentration and dye concentration at time t_i, respectively. V_o and V_s (L) are the volume of the dye solution and that of the sample solution taken out each time for dye concentration analysis, respectively. In this equation, V_s is equal to 0.001 L. Finally, m (g) represents the mass of the adsorbent.

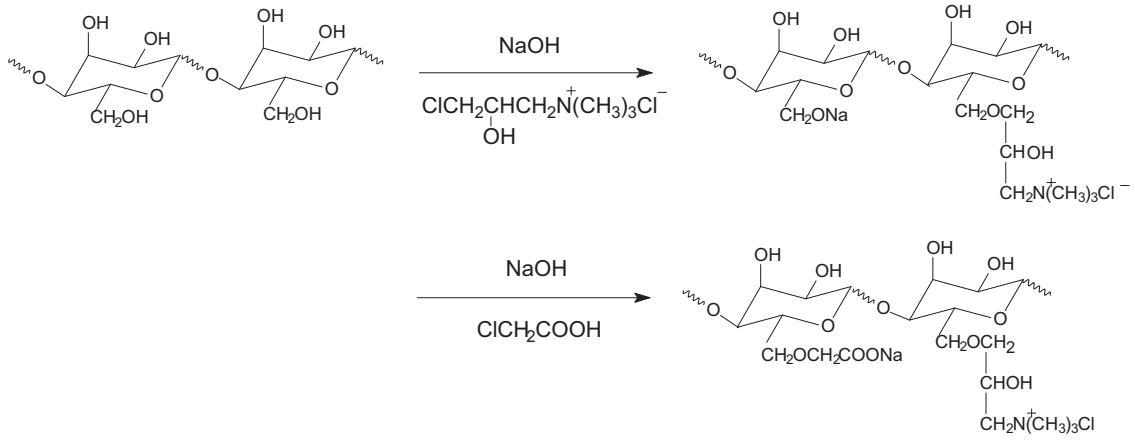

Scheme 1. Synthesis of AWS (cellulose as example).

2.5. Recycling experiments

The MB-loaded adsorbents were recovered from the 0.1 mol L^{-1} H_2SO_4 aqueous solution, and then collected from the solutions via filtration, washed with distilled water, and then reused in the next cycle of adsorption experiments. Similarly, the AG25-loaded adsorbents were recovered from the 0.1 mol L^{-1} NaOH aqueous solution. The adsorption–desorption experiments were conducted for six cycles. All experiments were performed at room temperature.

3. Results and discussion

3.1. Characterization of the biosorbent

Scheme 1 describes the preparation process of the amphoteric straw-based adsorbent. The quaternary ammonium and carboxymethyl groups were successively introduced to the straw. FTIR technique was employed to identify the molecular structure of the material. Besides AWS, the FTIR spectra of WS, a cationic straw (CTA-grafted straw), and an anionic straw (carboxymethylated straw) were measured and are shown in Fig. 1 for comparison. Fig. 1 shows that the characteristic peaks around 3337, 2903, and 1030 cm^{-1} appeared in all the straw materials, which were attributed to the stretch vibrations of O—H in the hydroxyl groups, C—H in the methylene groups, and C—O—C in the glucose rings of cellulose and lignin, respectively, because these polysaccharide materials are abundant in straw. However, the extra peaks at 1479 cm^{-1} in the cationic straw and 1590 cm^{-1} in the anionic straw (shown in Fig. 1(b) and (c)) appeared and corresponded to the characteristic peaks of the quaternary ammonium and carboxyl groups, respectively, compared with WS. Moreover, both of the aforementioned peaks were found in AWS, as shown in Fig. 1(d), indicating that the cationic and anionic groups grafted onto the straw after modification.

Furthermore, the pH dependence of the ζ potential of AWS was measured and shown in Fig. 2. The pH dependence of the ζ potential of WS, the anionic straw, and the cationic straw were also measured for comparison. Fig. 2 shows that the ζ potential of anionic straw is lesser in the measured pH range, indicating negative charges on the surface of the material. By contrast, the ζ potential of the cationic straw is positive in all pH ranges due to the cationic quaternary ammonium groups. AWS has both cationic and anionic groups; thus, its ζ potential is higher than that of anionic straw, but lower than that of cationic straw. The isoelectric point is around 3.5. The carboxyl groups are mostly protonized, and the ζ potential of AWS is positive at pH lower than 3.5. On the other hand, the carboxyl groups begin to deprotonize, whereas the quaternary ammonium groups hydrate, resulting in the decrease of the ζ potential when pH is higher than 3.5. All the aforementioned characterization results confirm that the amphoteric straw-based adsorbent is prepared successfully.

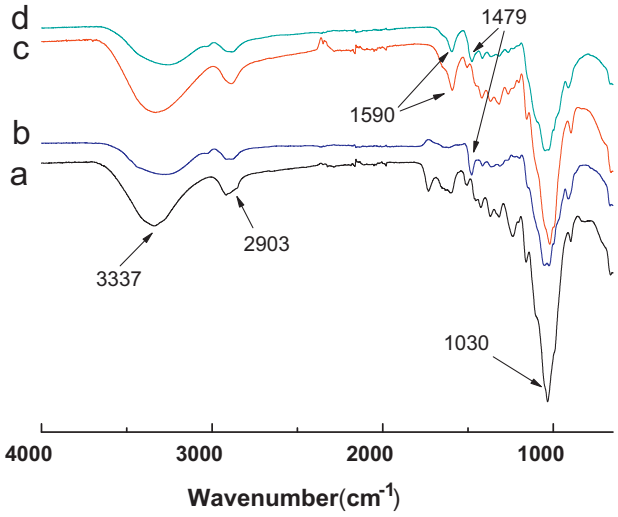

Fig. 1. FTIR spectra of WS (a), cationic straw (b), anionic straw (c), and AWS (d).

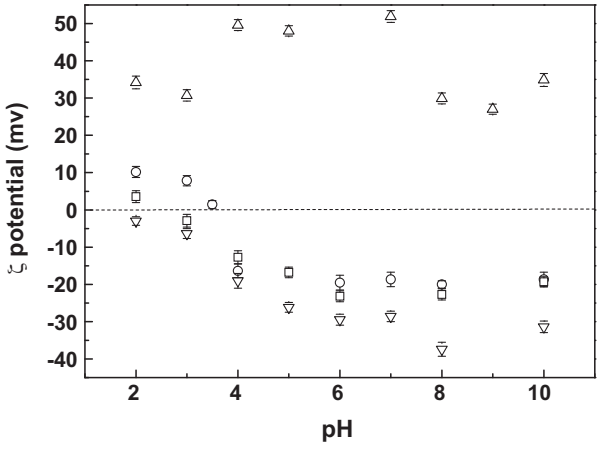

Fig. 2. The ζ potentials of WS (□), cationic straw (△), anionic straw (▽), and AWS (○) at varied pH conditions.

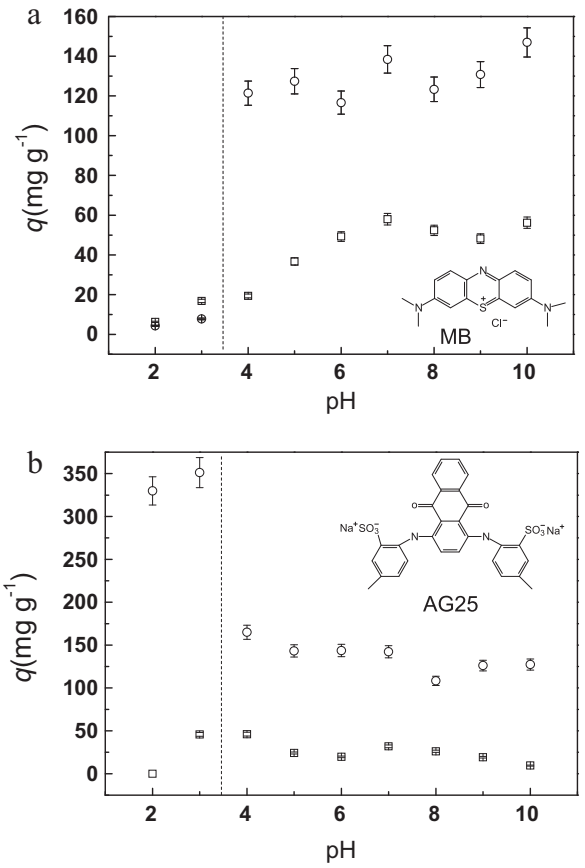

Fig. 3. The effects of pH on MB (a) and AG25 (b) adsorption by WS (□) and AWS (○) at 298 K, respectively.

Then, colloidal titration is applied to determine the amounts of quaternary ammonium and carboxymethyl groups that have been successfully impregnated onto the straw surface. Results show that one gram of AWS contains 0.644 mmol quaternary ammonium groups and 0.736 mmol carboxymethyl groups, respectively.

3.2. pH effects on the adsorption of various dyes

Among all the factors that might influence the adsorption capacity of ionic-type adsorbents, pH is one of the most important factors. Thus, the pH effects on MB and AG25 adsorption by AWS have been investigated. A clear boundary at pH of approximately 3.5 could be observed in both Fig. 3(a) and (b). The adsorption capacity of AG25 is considerable, whereas that of MB is comparatively low at pH lower than 3.5. By contrast, the adsorption capacity of MB is satisfactory, whereas that of AG25 decreases largely at pH higher than 3.5. Coincidentally, this pH boundary is quite near the isoelectric point of AWS. In addition, Fig. 3 also shows that the maximum adsorption capacity of AWS took place at pH 10.0 for MB around 140 mg g^{-1} and 3.0 for AG25 around 360 mg g^{-1}. Based on the calculated amounts of quaternary ammonium and carboxymethyl groups on AWS as mentioned above, it is estimated that one MB ion might be adsorbed by approximately two carboxymethyl groups while one AG25 ion might be adsorbed by approximately one quaternary ammonium group.

For comparison, the adsorption capacities of MB and AG25 by other reported adsorbents are summarized in Table 1. Most of the maximum MB uptakes by various adsorbents were at neutral or alkaline condition, while AG25 adsorptions were mostly favored at pH near 3.0, which were full consistent with current study. In addition, AWS exhibited higher adsorption capacities than most reported adsorbents for both MB and AG25. Accordingly, AWS could be considered as a promising adsorbent for the removal of both cationic and anionic dyes.

However, the adsorption of ionic dyes onto the adsorbents is mainly based on electrostatic interaction. MB is a type of cationic dye that has good affinity with anionic matters. By contrast, AG25 is a kind of anionic dye that has fine affinity with cationic matters. The carboxyl groups on AWS are mostly protonized and the adsorption of MB is inhibited at low pH range. Meanwhile, the quaternary ammonium groups on AWS could bind with sulfonic groups of AG25 easily. However, the quaternary ammonium groups are gradually hydrolyzed, whereas the carboxyl groups deprotonize with increase in pH. Therefore, the AG25 uptakes decrease evidently for electrostatic repulsion, whereas MB is easily adsorbed for electrostatic interaction at high pH range. Fig. 3 shows that the adsorption capacities of AWS for both MB and AG25 are still higher than those of WS at all measured pH ranges.

3.3. Adsorption equilibrium study

Adsorption equilibrium studies were performed to understand further the adsorption process. According to Fig. 3, the maximum adsorption capacity of AWS took place at pH 10.0 for MB and 3.0 for AG25. Thus, the initial solution pH of MB and AG25 were adjusted at 10.0 and 3.0, respectively. The adsorption isotherms for MB and AG25 onto AWS at varied temperatures are presented in Supporting Information Fig. S1. As shown in Fig. S1, the adsorption isotherms for both MB and AG25 show no significant variations with temperature. This phenomenon indicates the absence of physical adsorption, which is usually notably affected by temperature.

The equilibrium adsorption data could be correlated to different isotherm models, such as Langmuir (1918), Freundlich (1907), Sips (1948), and Dubinin–Radushkevich (D–R) (Dubinin, 1947), for investigation of the adsorption mechanism. The representation of the adsorption equilibrium equations was shown in Supporting Information TEXT S1. The fitting parameters of the above models are listed in Table 2. Table 2 shows that most of the determination coefficients (R^2) of the Langmuir model exceed 0.99 for both MB and AG25 adsorption compared with those of the other models. This observation indicates that the Langmuir model is very suitable to describe the adsorption behavior for both dyes. Furthermore, the theoretical saturated adsorption capacities simulated using the Langmuir model are very close to the experimental results. The Langmuir model is based on an idealized assumption of identical adsorption heat and monolayer adsorption; thus, it is able to present the monolayer adsorption mechanism for both MB and AG25.

The fitting results of the Freundlich model are also listed in Table 2. Results show that the R^2 of the Freundlich model is much lower than that of Langmuir model. The Freundlich model is applied to describe a heterogeneous system. In the present research, the lower R^2 further support the monolayer adsorption mechanism.

The fitting parameters of the Sips model are also showed in Table 2. The R^2 of this model is lower than that of the Langmuir model, but still higher than that of the Freundlich model. Based on Eq. (S3) listed in Supporting Information, the adsorbent is heterogeneous if the heterogeneity factor (n^{-1}) is less than one. The Sips model would reduce to Langmuir equation if it has relatively homogenous binding sites when n^{-1} is close to or even 1.0. Table 2 shows that the calculated values of n^{-1} are all close to 1.0, which further indicates that AWS is a homogeneous adsorbent for both dyes.

The D–R model could also provide valuable information about adsorption mechanisms, physical or chemical processes, from the mean energy of adsorption (E). The adsorption behavior is described as physical adsorption when E is between 1.0 and

Table 1
Adsorption capacities of various adsorbents for MB and AG25.

Dyes	Adsorbents	Optimal pH	C_0 (mg L^{-1})	q (mg g^{-1})	Reference
MB	AWS	10.0	500	138.0–151.7	This study
MB	Active carbon	6.0	250	16.43	(Karagoz, Tay, Ucar, & Erdem, 2008)
MB	Carbon nanotube	7.0	40	35.4–64.7	(Yao, Xu, Chen, Xu, & Zhu, 2010)
MB	Fuel oil fly ash	7.0	1000	47	(Andini, Cioffi, Colangelo, Montagnaro, & Santoro, 2008)
MB	Hazelnut shell	9.0	100	19.3	(Dogan, Abak, & Alkan, 2009)
MB	Polymer containing β-cyclodextrin and carboxyl	7.0	85	64	(Zhao et al., 2009)
MB	Rice bran	6.0	80	55	(Wang, Zhou, Jiang, & Sun, 2008)
MB	Active carbon	9.0	1500	315.0	(Deng, Yang, Tao, & Dai, 2009)
AG25	AWS	3.0	600	353.0–371.5	This study
AG25	Chitosan	4.0	1000	645.1	(Wong, Szeto, Cheung, & McKay, 2004)
AG25	Date stones	2.5	2000	36.90	(Mahmoodi, Hayati, & Arami, 2010)
AG25	Durian peel	2.0	500	63.29	(Hameed & Hakimi, 2008)
AG25	Shells of bittim	2.0	40	16	(Aydin & Baysal, 2006)
AG25	Activated palm ash	2.0	600	123.4	(Hameed, Ahmad, & Aziz, 2007)
AG25	Sodium alginate/titania nanoparticle	2.0	500	151.5	(Mahmoodi, Hayati, Arami, & Bahrami, 2011)
AG25	Modified starch	4.0	800	1119	(Wang, Xiang, Cheng, & Li, 2010)

Table 2
The isotherms parameters for MB and AG25 adsorption onto amphoteric straw, respectively.

Dyes	pH	T (K)	q_{exp} (mg g^{-1})	Langmuir model			Freundlich model			Sips model				D–R model	
				q_L (mg g^{-1})	b_L (L g^{-1})	R^2	K_F	n	R^2	q_m (mg g^{-1})	b (L mg^{-1})	n	R^2	E (kJ mol^{-1})	R^2
MB	10.0	283	139.4	135.3	174.7	0.9965	30.12	3.252	0.7926	138.4	0.1210	0.8099	0.9219	11.27	0.8565
		293	132.2	133.0	93.91	0.9977	26.11	3.122	0.8359	133.4	0.09183	0.9832	0.9661	11.36	0.8955
		303	135.9	134.6	123.1	0.9967	27.24	3.086	0.7778	136.5	0.09795	0.8062	0.9248	11.60	0.8467
		313	138.0	140.3	77.32	0.9955	22.58	2.783	0.8248	139.5	0.07221	0.8152	0.9496	11.37	0.8814
AG25	3.0	283	397.7	370.4	73.99	0.9912	54.67	2.839	0.8079	389.3	0.04811	0.8178	0.9502	10.06	0.8936
		293	379.4	414.9	17.67	0.9944	27.05	2.182	0.8605	401.8	0.01960	0.9126	0.9680	8.841	0.9282
		303	354.0	373.1	20.17	0.9899	32.66	2.495	0.9465	410.1	0.01421	1.1096	0.9583	10.21	0.9657
		313	365.1	363.6	35.12	0.9939	41.87	2.697	0.9269	408.3	0.02262	1.2759	0.9728	10.96	0.9745

8.0 kJ mol^{-1}, whereas it is considered as a chemical adsorption when E is more than 8.0 kJ mol^{-1}. Table 2 shows that the calculated E for both dyes are all higher than 8.0 kJ mol^{-1}, indicating that the adsorption behavior follows the chemical adsorption process. This phenomenon might result in no significant variations with temperature of the adsorption behavior of AWS, as mentioned above.

3.4. Adsorption kinetics

Aside from the adsorption equilibrium study, adsorption kinetics was also performed to establish the time dependence of the adsorption. The experimental results of MB and AG25 adsorption on AWS versus time at different temperatures are shown in Supporting Information Fig. S2. As in Fig. S2, the adsorption equilibrium for MB is quickly achieved within 20 min, indicating a very fast adsorption rate. The adsorption is a little slower for AG25, but the adsorption equilibrium is still achieved within 60 min.

To study the time dependence of adsorption process and further investigate the adsorption mechanisms, four common kinetic models were used to fit the data, namely pseudo-first order (Lagergren, 1898), pseudo-second order (Ho & McKay, 1998), the Elovich equation (Low, 1960), and intraparticle diffusion models (Yahaya, Don, & Bhatia, 2009). The representation of kinetics equations is shown in Supporting Information TEXT S2 and the fitted parameters of these kinetic models are listed in Table 3. From the R^2 of the linear form for the various models shown in Table 3, the pseudo-second order model is found to be more suitable than the pseudo-first order model and intraparticle diffusion model to describe the adsorption kinetic behavior for both dyes. This phenomenon indicates that chemisorption, instead of physisorption or intraparticle diffusion, is the rate-controlling mechanism for the adsorption of both MB and AG25. The results are fully consistent with those drawn from the adsorption isotherm analysis. Moreover, the R^2 of the Elovich model all exceed 0.95, indicating the suitability of this model. The Elovich model has been successfully used to describe the adsorption kinetics of ion exchange systems. Thus, the adsorption behavior of MB

Table 3
The kinetic parameters for MB and AG25 adsorption onto amphoteric straw, respectively.

Dyes	pH	T (K)	q_{exp} (mg g^{-1})	Pseudo-first order model		Pseudo-second order model		Elovich model			Intraparticle diffusion model	
				k_1 (s^{-1})	R^2	k_2 (10^{-3} min^{-1})	R^2	A_E	B_E	R^2	k_p (mg g^{-1} min$^{-0.5}$)	R^2
MB	10.0	283	151.7	0.09269	0.9878	3.612	0.9998	90.32	16.97	0.9587	8.424	0.8481
		293	138.0	0.1865	0.9792	3.997	0.9992	60.84	28.17	0.9782	24.77	0.8843
		303	143.5	0.1923	0.9196	5.457	0.9995	64.96	30.04	0.9780	33.78	0.8687
		313	138.3	0.2050	0.9817	9.307	0.9996	102.3	12.30	0.9888	24.26	0.9538
AG25	3.0	283	367.6	0.03781	0.9821	0.1057	0.9900	33.86	86.02	0.9625	39.04	0.8932
		293	362.2	0.05256	0.9189	0.2022	0.9946	9.60	87.69	0.9716	38.70	0.8807
		303	353.0	0.04466	0.9403	0.2176	0.9981	32.45	76.17	0.9850	44.23	0.8834
		313	371.5	0.04922	0.9405	0.2774	0.9936	22.62	85.75	0.9798	48.89	0.8707

Table 4
Batch adsorption–desorption cycles of MB and AG25, respectively.

Cycle	MB		AG25	
	q_e (mg g^{-1})	Recovery (%)	q_e (mg g^{-1})	Recovery (%)
1	135.2	97.98	355.0	98.01
2	133.2	96.49	361.2	99.73
3	135.8	98.44	354.9	97.99
4	132.5	96.03	357.2	98.63
5	134.2	97.22	354.3	97.83
6	131.5	95.28	351.6	97.07

and AG25 on AWS is not only chemisorptions, but also ion exchange reactions.

3.5. Recycling experiments

Reusability is very important in developing a novel adsorbent for use in practical applications. Therefore, in the current work, the adsorption and desorption processes were repeated for six cycles to examine the potential of the amphoteric adsorbent. The MB-loaded and AG25-loaded adsorbents were recovered from 0.1 mol L^{-1} H_2SO_4 and 0.1 mol L^{-1} NaOH aqueous solutions, respectively, as described in detail in Section 2.5. Table 4 shows the experimental results of the adsorption capacities and the regeneration efficiency in each adsorption–desorption cycle. The experimental results indicate that the desorption of both MB and AG25 is thorough and the adsorption capacity of the regenerated adsorbent is almost unaffected. Furthermore, the high regeneration efficiency also illuminates that the quaternary ammonium and carboxymethyl groups on AWS is stable enough, and the amphoteric straw-based adsorbent is suitable for practical applications.

4. Conclusions

The new amphoteric straw-based material is efficient in removing both cationic and anionic dyes from aqueous solutions for tailoring multifunctional groups onto the adsorbent. The adsorption capacities of AWS for MB and AG25 are considerable. Furthermore, the dye-loaded adsorbent could be regenerated easily and the dye uptakes of the regenerated adsorbent are almost without any loss for a few cycles. Therefore, the amphoteric adsorbent is a promising material for practical applications in wastewater treatment. In addition, the adsorption equilibrium and kinetics study indicate that the adsorption behavior of AWS follows the monolayer chemical adsorption with an ion-exchange process.

Acknowledgments

This work is supported by the Natural Science Foundation of China (Grant No. 51073077, 50938004 and 50825802), the Open Fund from State Key Laboratory of Pollution Control and Resource Reuse of Nanjing University (Grant No. PCRRF11004), and the Fundamental Research Funds for the Central Universities (Grant No. 1105020504 and 1116020510).

Appendix A. Supplementary data

Supplementary data associated with this article can be found, in the online version, at http://dx.doi.org/10.1016/j.carbpol.2012.06.015.

References

Abdel-Aal, S. E., Gad, Y. H., & Dessouki, A. M. (2006). Use of rice straw and radiation-modified maize starch/acrylonitrile in the treatment of wastewater. *Journal of Hazardous Materials*, *129*(1–3), 204–215.

Andini, S., Cioffi, R., Colangelo, F., Montagnaro, F., & Santoro, L. (2008). Adsorption of chlorophenol, chloroaniline and methylene blue on fuel oil fly ash. *Journal of Hazardous Materials*, *157*(2–3), 599–604.

Aydin, H., & Baysal, G. (2006). Adsorption of acid dyes in aqueous solutions by shells of bittim (Pistacia khinjuk Stocks). *Desalination*, *196*(1–3), 248–259.

Binod, P., Sindhu, R., Singhania, R. R., Vikram, S., Devi, L., Nagalakshmi, S., et al. (2010). Bioethanol production from rice straw: An overview. *Bioresource Technology*, *101*(13), 4767–4774.

Deng, H., Yang, L., Tao, G. H., & Dai, J. L. (2009). Preparation and characterization of activatedcarbon from cottonstalk by microwave assisted chemical activation—Application in methylene blue adsorption from aqueous solution. *Journal of Hazardous Materials*, *166*(2–3), 1514–1521.

Dogan, M., Abak, H., & Alkan, M. (2009). Adsorption of methylene blue onto hazelnut shell: Kinetics, mechanism and activation parameters. *Journal of Hazardous Materials*, *164*(1), 172–181.

Dubinin, M. M. (1947). Sorption and structure of active carbons: I. Adsorption of organic vapors. *Zhurnal Fizicheskoi Khimii*, *21*, 1351.

Freundlich, H. (1907). Ueber die Adsorption in Loesun. *Zeitschrift fur Physikalische Chemie*, *57*, 385–470.

Gong, R., Jin, Y., Chen, F., Chen, J., & Liu, Z. (2006). Enhanced malachite green removal from aqueous solution by citric acid modified rice straw. *Journal of Hazardous Materials B*, *137*, 865–870.

Gong, R., Zhong, K., Hu, Y., Chen, J., & Zhu, G. (2008). Thermochemical esterifying citric acid onto lignocellulose for enhancing methylene blue sorption capacity of rice straw. *Journal of Environmental Management*, *88*(4), 875–880.

Hameed, B. H., Ahmad, A. A., & Aziz, N. (2007). Isotherms, kinetics and thermodynamics of acid dye adsorption on activated palm ash. *Chemical Engineering Journal*, *133*(1–3), 195–203.

Hameed, B. H., & Hakimi, H. (2008). Utilization of durian (Durio zibethinus Murray) peel as low cost sorbent for the removal of acid dye from aqueous solutions. *Biochemical Engineering Journal*, *39*(2), 338–343.

Ho, Y. S., & McKay, G. (1998). Sorption of dye from aqueous solution by peat. *Chemical Engineering Journal*, *70*(2), 115–124.

Hou, Q. X., Yang, B., Liu, W., Liu, H. B., Hong, Y. M., & Zhang, R. X. (2011). Co-refining of wheat straw pulp and hardwood kraft pulp. *Carbohydrate Polymers*, *86*(1), 255–259.

Ibrahim, S., Fatimah, I., Ang, H. M., & Wang, S. B. (2010). Adsorption of anionic dyes in aqueous solution using chemically modified barley straw. *Water Science and Technology*, *62*(5), 1177–1182.

Ibrahim, S., Shuy, W. Z., Ang, H. M., & Wang, S. B. (2010). Preparation of bioadsorbents for effective adsorption of a reactive dye in aqueous solution. *Asia-Pacific Journal of Chemical Engineering*, *5*(4), 563–569.

Karagoz, S., Tay, T., Ucar, S., & Erdem, M. (2008). Activated carbons from waste biomass by sulfuric acid activation and their use on methylene blue adsorption. *Bioresource Technology*, *99*(14), 6214–6222.

Khan, M. M. R., Ray, M., & Guha, A. K. (2011). Mechanistic studies on the binding of Acid Yellow 99 on coir pith. *Bioresource Technology*, *102*(3), 2394–2399.

Kuang, X., Kuang, R., Zheng, X. D., & Wang, Z. L. (2010). Mechanical properties and size stability of wheat straw and recycled LDPE composites coupled by waterborne coupling agents. *Carbohydrate Polymers*, *80*(3), 927–933.

Lagergren, S. (1898). About the theory of so-called adsorption of soluble substances. *Kungliga Svenska vetenskapsakademiens Handlingar*, *24*, 1–39.

Langmuir, I. (1918). The adsorption of gases on plane surfaces of glass, mica and platinum. *Journal of the American Chemical Society*, *40*, 1361–1403.

Li, X. G., Wang, S. X., Duan, L., Hao, J., Li, C., Chen, Y. S., et al. (2007). Particulate and trace gas emissions from open burning of wheat straw and corn stover in China. *Environmental Science & Technology*, *41*(17), 6052–6058.

Low, M. J. D. (1960). Kinetics of chemisorption of gases on solids. *Chemical Reviews*, *60*(3), 267–312.

Mahmoodi, N. M., Hayati, B., & Arami, M. (2010). Textile dye removal from single and ternary systems using date stones: Kinetic, isotherm, and thermodynamic studies. *Journal of Chemical and Engineering Data*, *55*(11), 4638–4649.

Mahmoodi, N. M., Hayati, B., Arami, M., & Bahrami, H. (2011). Preparation, characterization and dye adsorption properties of biocompatible composite (alginate/titania nanoparticle). *Desalination*, *275*(1–3), 93–101.

Ngah, W. S. W., Teong, L. C., & Hanafiah, M. (2011). Adsorption of dyes and heavy metal ions by chitosan composites: A review. *Carbohydrate Polymers*, *83*(4), 1446–1456.

Oei, B. C., Ibrahim, S., Wang, S., & Ang, H. M. (2009). Surfactant modified barley straw for removal of acid and reactive dyes from aqueous solution. *Bioresource Technology*, *100*(18), 4292–4295.

O'Neill, C., Hawkes, F. R., Hawkes, D. L., Lourenco, N. D., Pinheiro, H. M., & Delee, W. (1999). Colour in textile effluents – sources, measurement, discharge consents and simulation: A review. *Journal of Chemical Technology and Biotechnology*, *74*(11), 1009–1018.

Rafatullah, M., Sulaiman, O., Hashim, R., & Ahmad, A. (2010). Adsorption of methylene blue on low-cost adsorbents: A review. *Journal of Hazardous Materials*, *177*(1–3), 70–80.

Serpone, N., Horikoshi, S., & Emeline, A. V. (2010). Microwaves in advanced oxidation processes for environmental applications. A brief review. *Journal of Photochemistry and Photobiology C: Photochemistry Reviews*, *11*(2–3), 114–131.

Sips, R. (1948). On the structure of a catalyst surface. *Journal of Chemical Physics*, *16*(5), 490–495.

Sonawane, G. H., & Shrivastava, V. S. (2009). Kinetics of decolourization of malachite green from aqueous medium by maize cob (zea maize): An agricultural solid waste. *Desalination*, *247*(1–3), 430–441.

Tanyildizi, M. S. (2011). Modeling of adsorption isotherms and kinetics of reactive dye from aqueous solution by peanut hull. *Chemical Engineering Journal*, *168*(3), 1234–1240.

Tsai, W. T., Hsu, H. C., Su, T. Y., Lin, K. Y., Lin, C. M., & Dai, T. H. (2007). The adsorption of cationic dye from aqueous solution onto acid-activated andesite. *Journal of Hazardous Materials*, *147*(3), 1056–1062.

Vandevivere, P. C., Bianchi, R., & Verstraete, W. (1998). Treatment and reuse of wastewater from the textile wet-processing industry: Review of emerging technologies. *Journal of Chemical Technology and Biotechnology*, *72*(4), 289–302.

Wang, G., Kawamura, K., Xie, M., Hu, S., Cao, J., An, Z., et al. (2009). Organic molecular compositions and size distributions of Chinese summer and autumn aerosols from Nanjing: Characteristic haze event caused by wheat straw burning. *Environmental Science & Technology*, *43*(17), 6493–6499.

Wang, X. S., Zhou, Y., Jiang, Y., & Sun, C. (2008). The removal of basic dyes from aqueous solutions using agricultural by-products. *Journal of Hazardous Materials*, *157*(2–3), 374–385.

Wang, Z. H., Xiang, B., Cheng, R. M., & Li, Y. J. (2010). Behaviors and mechanism of acid dyes sorption onto diethylenetriamine-modified native and enzymatic hydrolysis starch. *Journal of Hazardous Materials*, *183*(1–3), 224–232.

Wong, Y. C., Szeto, Y. S., Cheung, W. H., & McKay, G. (2004). Adsorption of acid dyes on chitosan – equilibrium isotherm analyses. *Process Biochemistry*, *39*(6), 693–702.

Xu, X., Gao, B. Y., Yue, Q. Y., & Zhong, Q. Q. (2010). Preparation and utilization of wheat straw bearing amine groups for the sorption of acid and reactive dyes from aqueous solutions. *Journal of Hazardous Materials*, *182*(1–3), 1–9.

Yahaya, Y. A., Don, M. M., & Bhatia, S. (2009). Biosorption of copper (II) onto immobilized cells of *Pycnoporus sanguineus* from aqueous solution: Equilibrium and kinetic studies. *Journal of Hazardous Materials*, *161*(1), 189–195.

Yao, Y. J., Xu, F. F., Chen, M., Xu, Z. X., & Zhu, Z. W. (2010). Adsorption behavior of methylene blue on carbon nanotubes. *Bioresource Technology*, *101*(9), 3040–3046.

Yu, J. X., Chi, R. A., He, Z. Y., & Qi, Y. F. (2011). Adsorption performances of cationic dyes from aqueous solution on pyromellitic dianhydride modified sugarcane bagasse. *Separation Science and Technology*, *46*(3), 452–459.

Zahrim, A. Y., Tizaoui, C., & Hilal, N. (2011). Coagulation with polymers for nanofiltration pre-treatment of highly concentrated dyes: A review. *Desalination*, *266*(1–3), 1–16.

Zhang, W. X., Yan, H., Li, H. J., Jiang, Z. W., Dong, L., Kan, X. W., et al. (2011). Removal of dyes from aqueous solutions by straw based adsorbents: Batch and column studies. *Chemical Engineering Journal*, *168*(3), 1120–1127.

Zhang, Y. X., Tao, S., Cao, J., & Coveney, R. M. (2007). Emission of polycyclic aromatic hydrocarbons in China by county. *Environmental Science & Technology*, *41*(3), 683–687.

Zhao, D., Zhao, L., Zhu, C. S., Shen, X. Y., Zhang, X. Z., & Sha, B. F. (2009). Comparative study of polymer containing β-cyclodextrin and -COOH for adsorption toward aniline, 1-naphthylamine and methylene blue. *Journal of Hazardous Materials*, *171*(1–3), 241–246.